On the Spectral Dynamics of Noise-Seeded Modulation Instability in Optical Fibers

P.I. Fierens, S.M. Hernandez, J. Bonetti and D.F. Grosz

Abstract We revisit modulation instability in optical fibers, including all relevant effects, such as higher-order dispersion terms, self-steepening, and the Raman response. Our analysis allows us to calculate the spectral evolution of a small perturbation to a continuous pump, and thus obtain an analytical expression for the small-signal spectral dynamics, showing excellent agreement with numerical simulations. We apply the expression for the spectral evolution to the case of white Gaussian noise and calculate some relevant metrics of the resulting signal, such as its coherence and signal-to-noise ratio. These calculations might shed some light on the nonlinear phenomena of supercontinuum generation.

1 Introduction

The phenomenon of modulation instability (MI) has been known and thoroughly studied for many years in a vast number of different areas of science, see e.g. [1–4], just to cite a few. In the realm of optical fibers [5, 6], in particular, MI plays a fundamental role as it is intimately connected to the appearance of optical solitons, which have had a strong impact on applications to high-capacity fiber optics communication. In recent years, nonlinear phenomena such as supercontinuum generation [7] and rogue waves [8] in optical fibers have rekindled the interest in MI. Supercontinuum generation refers to the phenomenon by which a narrowband input to an optical

P.I. Fierens (✉)
Instituto Tecnológico de Buenos Aires (ITBA) and Consejo Nacional
de Investigaciones Científicas Y Técnicas (CONICET), Buenos Aires, Argentina
e-mail: pfierens@itba.edu.ar

S.M. Hernandez
Instituto Balseiro (IB), Bariloche, Argentina

J. Bonetti
IB, Bariloche, Argentina

D.F. Grosz
IB and CONICET, Buenos Aires, Argentina

fiber, such as a continuous wave, spreads to become a wideband signal, comprising several octaves, due to the fiber nonlinearity. Rogue waves, also known as freak waves, are high-amplitude pulses which occur with very low probability. These rare pulses have been studied in several areas, including oceanography, where they are associated to large waves that 'appear from nowhere'.

In Sect. 2, we tackle the problem of the spectral evolution of a small perturbation to a continuous wave. Our results include molecular Raman scattering and higher orders of the nonlinearity, such as self-steepening. To the best of our knowledge, such a complete description has been only presented by Béjot et al. [9] in a more general context.

In Sect. 3, we apply the results on spectral dynamics to the case of additive white Gaussian noise and relate it to the generation of supercontinua. We must observe that the relation between MI and supercontinuum generation has been extensively studied in the literature (see, e.g., [7, 10–18]). The literature on the influence of diverse noise sources on modulation instability, supercontinua and rogue waves is also extensive (see, e.g., [19–25] and references therein). In this work, we derive some interesting formulas on the relation of modulation instability and some metrics such as coherence [7] and signal-to-noise ratio [26, 27]. Although these results are limited to the undepleted pump and perturbative approximations, they might provide some insight on the onset of supercontinuum generation.

2 Spectral Dynamics of Modulation Instability

Wave propagation in a lossless optical fiber can be described by the generalized nonlinear Schrödinger equation [28],

$$\frac{\partial A}{\partial z} - i\hat{\beta}A = i\hat{\gamma}A(z,T)\int_{-\infty}^{+\infty} R(T')\left|A(z,T-T')\right|^2 dT', \tag{1}$$

where $A(z,T)$ is the slowly-varying envelope, z is the spatial coordinate, and T is the time coordinate in a comoving frame at the group velocity ($=\beta_1^{-1}$). $\hat{\beta}$ and $\hat{\gamma}$ are operators related to the dispersion and nonlinearity, respectively, and are defined by

$$\hat{\beta} = \sum_{m\geq 2} \frac{i^m}{m!}\beta_m \frac{\partial^m}{\partial T^m},\ \hat{\gamma} = \sum_{n\geq 0} \frac{i^n}{n!}\gamma_n \frac{\partial^n}{\partial T^n}.$$

The β_m's are the coefficients of the Taylor expansion of the propagation constant $\beta(\omega)$ around a central frequency ω_0. In the convolution integral in the right hand side of Eq. (1), $R(T)$ is the nonlinear response function that includes both the instantaneous (electronic) and delayed Raman response.

We shall analyze the effect of a small perturbation a to the stationary solution A_s of Eq. (1) (see [28])

$$A(z,T) = \left(\sqrt{P_0} + a\right) e^{i\gamma_0 P_0 z} = A_s + a e^{i\gamma_0 P_0 z}. \tag{2}$$

If we keep only terms linear in the perturbation, after some manipulations, substitution of Eq. (2) into Eq. (1) leads to

$$\frac{\partial \tilde{a}(z,\Omega)}{\partial z} + \tilde{N}(\Omega)\tilde{a}(z,\Omega) = \tilde{M}(\Omega)\tilde{a}^*(z,-\Omega), \tag{3}$$

where $\Omega = \omega - \omega_0$, $\tilde{a}$, $\tilde{\beta}$, $\tilde{\gamma}$, and $\tilde{R}$ are the Fourier transforms of a, β, γ and R, respectively. Moreover, for the sake of clarity we have defined

$$\tilde{N}(\Omega) = -i\left[\tilde{\beta}(\Omega) + P_0\tilde{\gamma}(\Omega)\left(1+\tilde{R}(\Omega)\right) - P_0\gamma_0\right], \tag{4}$$

$$\tilde{M}(\Omega) = iP_0\tilde{\gamma}(\Omega)\tilde{R}(\Omega). \tag{5}$$

After some straightforward algebra and using the ansatz $a(z,\Omega) = D\exp(iK(\Omega)z)$, the following dispersion relation is found

$$K(\Omega) = -\tilde{B}(\Omega) \pm \sqrt{\tilde{B}^2(\Omega) - \tilde{C}(\Omega)}, \tag{6}$$

where

$$\tilde{B}(\Omega) = -\left[\tilde{\beta}_o(\Omega) + P_0\tilde{\gamma}_o(\Omega)\left(1+\tilde{R}(\Omega)\right)\right], \tag{7}$$

$$\begin{aligned}\tilde{C}(\Omega) = {} & \tilde{\beta}_o^2(\Omega) - \tilde{\beta}_e^2(\Omega) + \\ & + P_0^2\left(\tilde{\gamma}_o^2(\Omega) - \tilde{\gamma}_e^2(\Omega)\right)\left(1+2\tilde{R}(\Omega)\right) - P_0^2\gamma_0^2 + \\ & + 2P_0\gamma_0\tilde{\beta}_e(\Omega) + 2P_0^2\gamma_0\tilde{\gamma}_e(\Omega)\left(1+\tilde{R}(\Omega)\right) + \\ & + 2P_0\left(\tilde{\beta}_o\tilde{\gamma}_o - \tilde{\beta}_e\tilde{\gamma}_e\right)\left(1+\tilde{R}(\Omega)\right),\end{aligned} \tag{8}$$

$$\tilde{\beta}_e(\Omega) = \sum_{n\geq 1}\frac{\beta_{2n}}{(2n)!}\Omega^{2n},\ \tilde{\beta}_o(\Omega) = \sum_{n\geq 1}\frac{\beta_{2n+1}}{(2n+1)!}\Omega^{2n+1}, \tag{9}$$

$$\tilde{\gamma}_e(\Omega) = \sum_{n\geq 0}\frac{\gamma_{2n}}{(2n)!}\Omega^{2n},\ \tilde{\gamma}_o(\Omega) = \sum_{n\geq 0}\frac{\gamma_{2n+1}}{(2n+1)!}\Omega^{2n+1}. \tag{10}$$

A simple expression can be obtained by setting $\gamma_n = 0$ for $n \geq 2$ and $\gamma_1 = \gamma_0\tau_{\mathrm{sh}}$ (accounting for the effect of self-steepening). In this case,

$$\begin{aligned}K(\Omega) = {} & \tilde{\beta}_o + P_0\gamma_0\tau_{\mathrm{sh}}\Omega\left(1+\tilde{R}\right) \pm \\ & \pm\sqrt{\left(\tilde{\beta}_e + 2\gamma_0 P_0\tilde{R}\right)\tilde{\beta}_e + P_0^2\gamma_0^2\tau_{\mathrm{sh}}^2\Omega^2\tilde{R}^2}.\end{aligned} \tag{11}$$

Expression (6) agrees with that in Ref. [9], and with the one with $\gamma_k = 0$ for $k \geq 1$ in Ref. [29]. As usual, the MI gain can be found as the imaginary part of $K(\Omega)$. The resulting equation exhibits many properties of the gain that have been thoroughly studied in the literature, for instance, the fact that it does not depend on odd terms of the dispersion relation (e.g., β_3) [6, 29]. However, the derived MI gain also reveals some interesting aspects related to the self-steepening term $\gamma_0 \tau_{\mathrm{sh}}$. Indeed, it already has been noted that this term enables a gain even in a zero-dispersion fiber and that, in general, leads to a narrowing of the MI gain bandwidth [30, 31].

Equation (11) also shows that, for large input power, the MI gain spectrum is dominated by the Raman response, *i.e.*,

$$|g(\Omega)| \approx 2P_0\gamma_0\tau_{\mathrm{sh}}|\Omega| \cdot \left|\mathrm{Im}\left\{\tilde{R}(\Omega)\right\}\right|. \tag{12}$$

Thus, in the large pump power limit, the modulation instability gain is independent of the dispersion parameters β_m. Moreover, Eq. (11) shows that, for some values of P_0, the MI gain displays two well-defined maxima, one corresponding to the Raman contribution and the other related to the first term in the square root. This two-maxima scenario may be of particular relevance, for instance, in the onset of supercontinuum generation. Indeed, it is well known that modulation instability causes the CW pump to break-up into pulses with a period given by the frequency by that of the MI gain peak. In the case of two maxima of similar amplitudes, there is a approximately the same probability of producing trains of pulses with any of the two corresponding periods. Randomness is a consequence of the amplification of the input noise.

To portray the influence of the various effects in the MI gain, Figs. 1 and 2 show two examples where the pump power is 100 W (Fig. 1) and 5 kW (Fig. 2), at a center wavelength of 5 μm. The dispersion and nonlinear parameters of the fiber are $\beta_2 = -1\,\mathrm{ps}^2/\mathrm{km}$, $\beta_2 = 0.04\,\mathrm{ps}^3/\mathrm{km}$, $\beta_4 = -0.0016\,\mathrm{ps}^4/\mathrm{km}$, $\gamma_0 = 100\,(\mathrm{W\,m})^{-1}$. Curves labeled G_3 and G_4 include the effect of self-steepening ($\tau_{\mathrm{sh}} = 1/\omega_0$). While

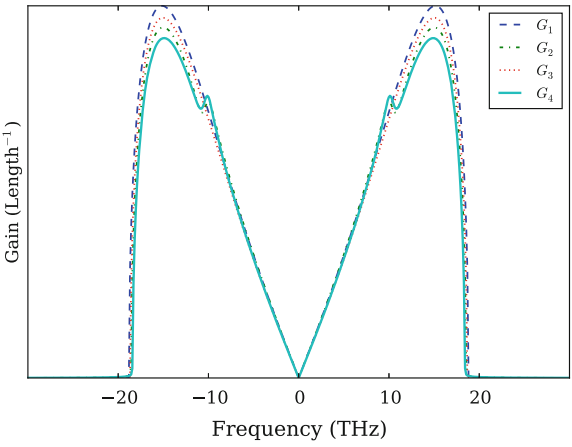

Fig. 1 MI Gain. Pump power: 100 W. G_3 and G_4 include the effect of the Raman response. G_2 and G_4 take into account the effect of self-steepening

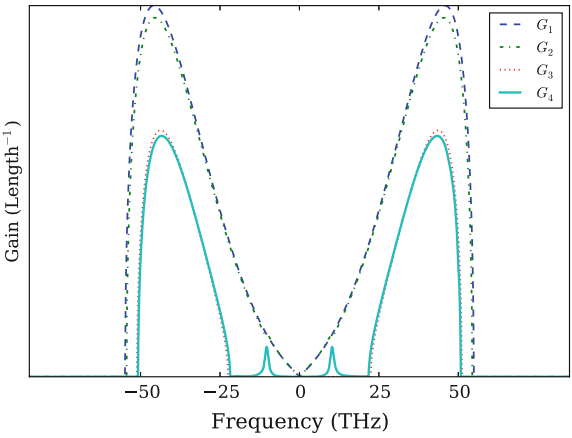

Fig. 2 MI Gain. Pump power: 5 kW. G_3 and G_4 include the effect of the Raman response. G_2 and G_4 take into account the effect of self-steepening

the nonlinear response is $R(T) = \delta(T)$ in curves labeled G_1 and G_3, in G_2 and G_4 the response $R(T) = (1 - f_R)\delta(T) + f_R h_R(T)$, with

$$h_R(T) = \frac{\tau_1^2 + \tau_2^2}{\tau_1 \tau_2^2} e^{-T/\tau_2} \sin(T/\tau_1) u(T),$$

where $u(T)$ is the Heaviside step function, $f_R = 0.031$, $\tau_1 = 15.5\,\text{fs}$, $\tau_2 = 230.5\,\text{fs}$ [32]. The chosen set of parameters correspond to those of a typical chalcogenide waveguide. We chose this particular medium as it is the most appropriate for applications in the mid IR, a region of singular interest in the are of molecular spectroscopy [33]. The influence of self-steepening reveals itself in the difference between curves G_1 and G_2 in Fig. 2. No relevant gain is observed when the Raman response is included, but self-steepening is neglected. Indeed, as seen in Eq. (12), in the large input power limit τ_{sh} acts as a 'switch', turning on and off the Raman response.

From Eqs. (2) and (6), the spectrum of the perturbation is given by

$$\tilde{a}(z, \Omega) = D_1(\Omega) e^{iK_1(\Omega)z} + D_2(\Omega) e^{iK_2(\Omega)z}, \tag{13}$$

where $K_1(\Omega)$ and $K_2(\Omega)$ are the solutions in Eq. (6) with the plus and the minus sign, respectively. $D_1(\Omega)$ and $D_2(\Omega)$ are functions that depend on the nature of the perturbation at the input end of the optical fiber. Letting $\tilde{a}(0, \Omega) = \Lambda(\Omega)$ in Eqs. (3) and (13), after some calculations we obtain

$$D_{1,2}(\Omega) = \frac{\tilde{M}(\Omega)\Lambda^*(-\Omega) - \left[\tilde{N}(\Omega) + iK_{2,1}(\Omega)\right]\Lambda(\Omega)}{i(K_{1,2}(\Omega) - K_{2,1}(\Omega))}. \tag{14}$$

Another useful way of writing Eqs. (13)–(14) is

$$\tilde{a}(z,\Omega) = \frac{e^{-i\tilde{B}(\Omega)z}}{K_D(\Omega)} \Big\{ \tilde{M}(\Omega)\sin(K_D(\Omega)z)A^*(-\Omega) + \\ + \Big[K_D(\Omega)\cos(K_D(\Omega)z) - \\ - \big(\tilde{N}(\Omega) - i\tilde{B}(\Omega)\big)\sin(K_D(\Omega)z) \Big] A(\Omega) \Big\}, \tag{15}$$

where $K_D(\Omega) = \sqrt{\tilde{B}^2(\Omega) - \tilde{C}(\Omega)}$. Similar expressions can be found in Ref. [9]. It is interesting to note that, in the case of a small harmonic signal $a(0,T) = \alpha \exp(i\Omega_0 T)$, these equations imply that a second harmonic appears at $-\Omega_0$. In contrast to this behavior, the optical fiber appears to respond as a linear time invariant system when the input perturbation is a real function (*i.e.*, $a(0,T) \in \mathbb{R}$). In this case, $A^*(-\Omega) = A(\Omega)$ and Eq. (13) becomes $\tilde{a}(z,\Omega) = \tilde{H}(\Omega,z)A(\Omega)$.

3 Noise as a Perturbation

Although Eqs. (13)–(15) are general and can be applied to any type of perturbation, in this work we focus on white Gaussian noise. This type of input perturbation is relevant in real applications where a typical laser has a finite signal-to-noise ratio. Figure 3 shows the simulated spectra of 200 noise realizations for two different fiber lengths (10 and 40 mm), with the same parameters as in Figs. 1 and 2. The input SNR is set to a realistic ∼28 dB. A fourth-order Runge-Kutta in the interaction picture method was used for the simulations [34]. Spectral dynamics, as given by Eq. (13), allow us to obtain an accurate estimate for the mean value of the power spectral density, as shown in Fig. 3 (top). A departure from the analytical model is observed (cf. Fig. 3 (bottom)) as propagation deeper into the fiber renders a non-negligible pump depletion.

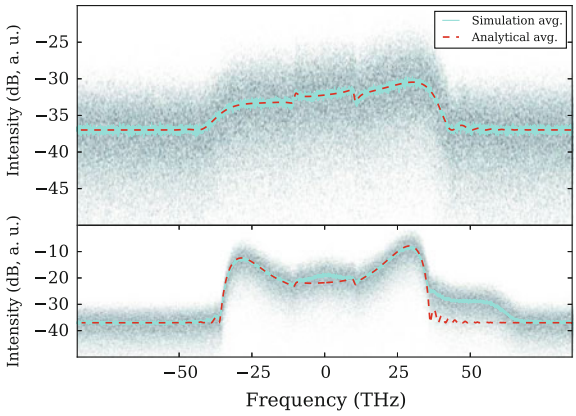

Fig. 3 Simulated spectral evolution of 200 noise realizations (background cloud of points), its average (*solid line*), and its corresponding analytical average (*dashed line*): @ 10 mm (*top*) and @ 40 mm (*bottom*)

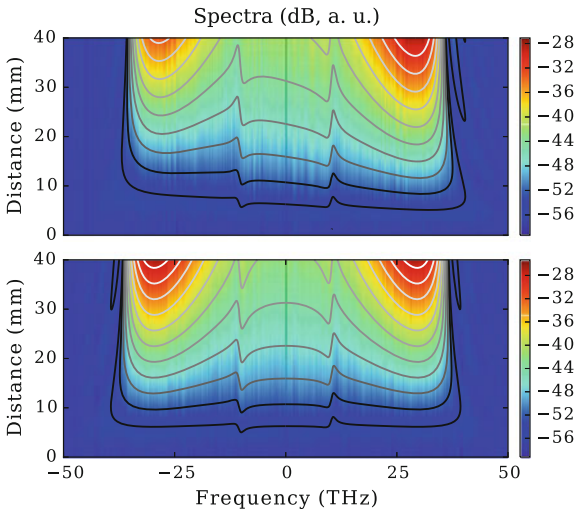

Fig. 4 Simulated spectral evolution of 50 noise realizations: with self-steepening (*top*) and without self-steepening (*bottom*). Contour plots correspond to simulated averages and solid lines to analytical mean values

It must be noted that our analysis incorporates higher orders of the nonlinear operator $\hat{\gamma}$, such as self-steepening. The relevance of this term can be observed in Fig. 4, where results with (top) and without (bottom) self-steepening are presented. All parameters are the same as in Fig. 3. Again, we find an excellent agreement between analytical results and numerical simulations. Moreover, spectral dynamics clearly depend on the inclusion of the self-steepening term.

We may study the AWGN case by considering $A(\Omega)$ as an independent circularly-symmetric normal random variable with variance σ^2 for each Ω, *i.e.*, $A(\Omega) \sim \mathcal{CN}(0, \sigma^2)$.[1] In this case, $A^*(-\Omega)$ is also an independent and identically distributed random variable. From Eq. (15), we know that $\tilde{a}(z, \Omega)$ is a linear combination of N_1 and N_2 and, hence, it is itself a circularly symmetric normal random variable, $\tilde{a}(z, \Omega) \sim \mathcal{CN}(0, \sigma_{\tilde{a}}^2)$. The variance $\sigma_{\tilde{a}}^2$ may be computed from Eq. (15) as

$$\begin{aligned}\sigma_{\tilde{a}}^2 =& \sigma^2 \left| \frac{e^{-i\tilde{B}(\Omega)z}}{K_D(\Omega)} \right|^2 \left\{ \left| \tilde{M}(\Omega) \sin(K_D(\Omega)z) \right|^2 + \right. \\ &\left. + \left| K_D(\Omega) \cos(K_D(\Omega)z) - \left(\tilde{N}(\Omega) - i\tilde{B}(\Omega) \right) \sin(K_D(\Omega)z) \right|^2 \right\}. \end{aligned} \tag{16}$$

Since $\tilde{a}(z, \Omega)$ is circularly symmetric, $|\tilde{a}(z, \Omega)| \sim \text{Rayleigh}(\sigma_{\tilde{a}})$ and $|\tilde{a}(z, \Omega)|^2 / \sigma_{\tilde{a}}^2$ has a χ^2-distribution with two degrees of freedom. Figure 5 shows a good agree-

[1] From a strict mathematical point of view, a process such as $A(\Omega)$ ($\Omega \in \mathbb{R}$) is not measurable (see, e.g., example 1.2.5 of is Ref. [35]). However, in simulations we deal only with a discrete set $\{\Omega_k\}_{k=0}^{N-1}$ for some finite integer N. Under a discrete setting, the definition of the process $A(\Omega_k)$ is correct. Since we will compare all our analytical results to simulations, we will stick to this definition of noise in the frequency domain and a more formal presentation will be published elsewhere.

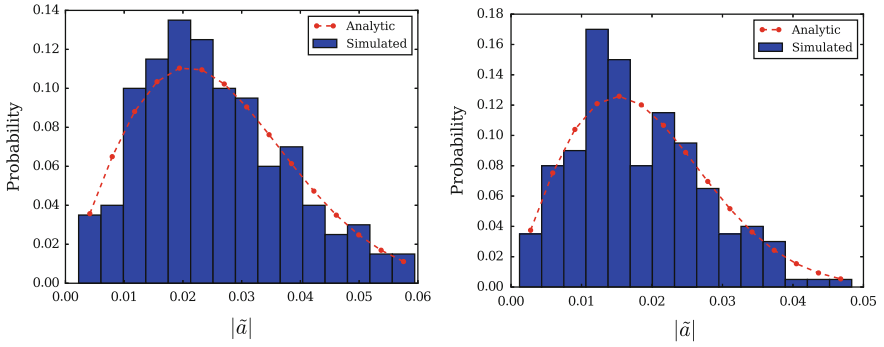

Fig. 5 Histograms of $|\tilde{a}(z, \Omega)|$ for $z = 10\,\text{mm}, f = 26.758\,\text{THz}$ (*left*) and $f = -26.758\,\text{THz}$ (*right*). Dashed lines correspond to the probabilities from a Rayleigh distribution with $\sigma_{\tilde{a}}$ calculated using Eq. (16)

ment between simulation results and these distributions. Simulation results are those shown also in Fig. 3.

It can be argued that, $a(z, t)$ must be a stationary process (at least in the wide-sense[2]) in t. Intuitively, it is the output of a time-invariant nonlinear system with a stationary input (CW pump + white noise).

An important metric in supercontinuum generation is the spectral coherence, defined as [7]

$$g_{12}(z, \Omega) = \frac{\left\langle \tilde{a}_k^*(z, \Omega)\tilde{a}_l(z, \Omega)\right\rangle_{k\neq l}}{\sqrt{\left\langle \left|\tilde{a}_k(z, \Omega)\right|^2\right\rangle \left\langle \left|\tilde{a}_l(z, \Omega)\right|^2\right\rangle}}, \tag{17}$$

where the subscripts k, l correspond to different noise realizations and the angle brackets denote ensemble averages. Since different realizations are independent and, from our results, $\tilde{a}_k(z, \Omega)$ are circularly symmetric normal random variables, the coherence is zero in the AWGN case. This result agrees well with previous observations, for example, in Ref. [26].

Another usual metric is the signal-to-noise ratio, defined in this context as [26, 27]

$$\text{SNR}(\Omega) = \frac{\left\langle |\tilde{a}(z, \Omega)|^2\right\rangle}{\sqrt{\text{Var}\left(|\tilde{a}(z, \Omega)|^2\right)}}, \tag{18}$$

where $\text{Var}(X) = \left\langle |X - \langle X\rangle|^2\right\rangle$. Since $|\tilde{a}(z, \Omega)|^2/\sigma_{\tilde{a}}^2$ has a χ^2-distribution with two degrees of freedom, $\text{SNR}(\Omega) = 1$ for all Ω.

[2] A proper proof of this fact needs a correct definition of the stochastic process $A(\Omega)$.

3.1 A Simple Case

In order to gain some insight on these formulas, let us apply them for the textbook case where $\beta_2 < 0$ (anomalous dispersion), $\beta_k = 0$ for $k > 2$, $\gamma_n = 0$ for $n > 0$, $\tilde{R}(\Omega) = 1$ and $K_D^I(\Omega) = \mathrm{Im}\{K_D(\Omega)\} \neq 0$ (net MI gain). We obtain

$$\sigma_{\tilde{a}}^2 = \sigma^2 \left\{ 1 + \left(\frac{2\gamma_0^2 P_0^2}{\left(K_D^I(\Omega)\right)^2} \right) \sinh^2(K_D^I(\Omega) z) \right\}. \tag{19}$$

Defining $\Omega_c = 4\gamma_0 P_0/|\beta_2|$ [28] and using (11),

$$\sigma_{\tilde{a}}^2 = \sigma^2 \left\{ 1 + \left[\frac{2\left(\frac{\Omega_c}{\Omega}\right)^4}{\left(\frac{\Omega_c}{\Omega}\right)^2 - 1} \right] \sinh^2 \left(z \frac{|\beta_2|\Omega^2}{2} \sqrt{\left(\frac{\Omega_c}{\Omega}\right)^2 - 1} \right) \right\}. \tag{20}$$

For $\Omega = \Omega_c/\sqrt{2}$ (corresponding to the maximum MI gain),

$$\sigma_{\tilde{a}}^2 = \sigma^2 \left\{ 1 + 4 \sinh^2 \left(\frac{z}{L_{\mathrm{NL}}} \right) \right\} \approx \sigma^2 \exp\left(2 \frac{z}{L_{\mathrm{NL}}} \right), \tag{21}$$

where L_{NL} is the nonlinear length conventionally defined as $L_{\mathrm{NL}} = (\gamma_0 P_0)^{-1}$, and the approximation is valid for $z \gg 0$. Equation (21) shows explicitly how the noise variance increases with distance.

Whenever there is not a net gain (Ω such that $K_D^I(\Omega) = 0$), we have

$$\sigma_{\tilde{a}}^2 = \sigma^2 \left\{ 1 + \left[\frac{2\left(\frac{\Omega_c}{\Omega}\right)^4}{1 - \left(\frac{\Omega_c}{\Omega}\right)^2} \right] \sin^2 \left(z \frac{|\beta_2|\Omega^2}{2} \sqrt{1 - \left(\frac{\Omega_c}{\Omega}\right)^2} \right) \right\}. \tag{22}$$

One relevant conclusion is that the variance is periodic in z. Moreover, there are fiber lengths for which the variance is equal to that of the input field.

Since it $a(z,t)$ is a wide-sense stationary process, $\sigma_{\tilde{a}}^2(\Omega)$ is the power spectral density. Thus, the Wiener-Khinchin theorem allows us to find the autocorrelation function $r_a(z,\tau) =< a(z,t)a^*(z,t-\tau) >$ by computing an inverse Fourier transform. Although this calculation can be done numerically, it is instructive to find an analytic approximation.

Such analytic approximation is simple when we consider the case of short distances (say, $z < L_{\mathrm{NL}}/2$). In this case,

$$\sigma_{\tilde{a}}^2 \approx \sigma^2 \left\{ 1 + 2 \left(\frac{z}{L_{\mathrm{NL}}} \right)^2 \right\}. \tag{23}$$

The variance increases quadratically with the distance, but the process is essentially white. Therefore, the correlation is

$$r_a(z,\tau) \approx \sigma^2 \left\{ 1 + 2\left(\frac{z}{L_{\mathrm{NL}}}\right)^2 \right\} \delta(\tau). \tag{24}$$

For other values of z, a rough analytic approximation can be obtained by approximating $\sigma_{\tilde{a}}^2(\Omega)$ with a linear combination of bell-shaped distributions,

$$\sigma_{\tilde{a}}^2 \approx \sigma^2 \left\{ 1 + \alpha_z \left[e^{-\frac{(\Omega-\Omega_z)^2}{W_z}} + e^{-\frac{(\Omega+\Omega_z)^2}{W_z}} \right] \right\}, \tag{25}$$

where α_z, Ω_z and W_z are conveniently chosen constants. It can be shown that, for large $z\,(>L_{\mathrm{NL}})$, $\Omega_z \approx \Omega_c/\sqrt{(2)}$ (the position of the maximum MI gain), $W_z \approx (|\beta_2|z)^{-1}$ and $\alpha_z \approx 8\sinh^2(z/L_{\mathrm{NL}})$ lead to reasonable approximations. Then, the autocorrelation is given by

$$r_a(z,\tau) \approx \sigma^2 \left\{ \delta(\tau) + \frac{8\sinh^2\left(\frac{z}{L_{\mathrm{NL}}}\right)}{\sqrt{\pi|\beta_2|z}} e^{-\frac{\tau^2}{4|\beta_2|z}} \cos\left(\frac{\Omega_c}{\sqrt{2}}\tau\right) \right\}. \tag{26}$$

As it can be readily seen, the coherence increases with z. Note that, as the coherence time increases, the correlation appears to be periodic. This periodicity reflects the breakup of the CW pump into pulses with a period $\propto \sqrt{2}/\Omega_c$.

The first term in (26) involves a Dirac's delta due to the unrealistic assumption of the white Gaussian input noise. Have we assumed an approximately white noise in the relevant frequency band, the first term would still correspond to a narrow pulse with a width of the order of the noise bandwidth B_N. In any case, the first term does not depend on z and corresponds to the input noise power. Thus, for large z, we may write

$$\mathrm{Var}(a(z,t)) \approx S_N \left\{ W_N + \frac{8\sinh^2\left(\frac{z}{L_{\mathrm{NL}}}\right)}{\sqrt{\pi|\beta_2|z}} \right\}, \tag{27}$$

where S_N is the input-noise spectral power density.

4 Conclusions

In summary, we obtained analytical expressions for the spectral evolution of a perturbation to a continuous pump propagating in an optical fiber, including all relevant effects such as high-order dispersion, Raman response, and self-steepening.

In particular, we tackled the problem of the evolution of white Gaussian noise, a relevant case as it deals with the finite signal-to-noise ratio of real laser sources. We verified our analytical results with simulations of supercontinuum generation in the mid-IR band, finding an excellent agreement. We also obtained closed expressions for relevant metrics in the generation of supercontinua such as the spectral coherence, the signal-to-noise ratio.

References

1. T.B. Benjamin, J.E. Feir, J. Fluid Mech. **27**, 417 (1967). doi:10.1017/S002211206700045X
2. A. Shabat, V. Zakharov, Sov. Phys. JETP **34**, 62 (1972)
3. V.E. Zakharov, Sov. Phys. JETP **35**, 908 (1972)
4. N. Akhmediev, V. Korneev, Theoret. Math. Phys. **69**(2), 1089 (1986)
5. K. Tai, A. Hasegawa, A. Tomita, Phys. Rev. Lett. **56**, 135 (1986). doi:10.1103/PhysRevLett.56.135
6. M.J. Potasek, Opt. Lett. **12**(11), 921 (1987). doi:10.1364/OL.12.000921
7. J.M. Dudley, G. Genty, S. Coen, Rev. Mod. Phys. **78**, 1135 (2006). doi:10.1103/RevModPhys.78.1135
8. D. Solli, C. Ropers, P. Koonath, B. Jalali, Nature **450**(7172), 1054 (2007)
9. P. Béjot, B. Kibler, E. Hertz, B. Lavorel, O. Faucher, Phys. Rev. A **83**, 013830 (2011). doi:10.1103/PhysRevA.83.013830
10. A. Demircan, U. Bandelow, Opt. Commun. **244**(1), 181 (2005)
11. M.H. Frosz, O. Bang, A. Bjarklev, Opt. Express **14**(20), 9391 (2006). doi:10.1364/OE.14.009391
12. T. Sylvestre, A. Vedadi, H. Maillotte, F. Vanholsbeeck, S. Coen, Opt. Lett. **31**(13), 2036 (2006). doi:10.1364/OL.31.002036
13. A. Demircan, U. Bandelow, Appl. Phys. B **86**(1), 31 (2007)
14. J.M. Dudley, J.R. Taylor (eds.), *Supercontinuum Generation in Optical Fibers* (Cambridge University Press, 2010)
15. J.M. Soto-Crespo, A. Ankiewicz, N. Devine, N. Akhmediev, JOSA B **29**(8), 1930 (2012)
16. J.H. Price, X. Feng, A.M. Heidt, G. Brambilla, P. Horak, F. Poletti, G. Ponzo, P. Petropoulos, M. Petrovich, J. Shi, M. Ibsen, W.H. Loh, H.N. Rutt, D.J. Richardson, Opt. Fiber Technol. **18**(5), 327 (2012). doi:10.1016/j.yofte.2012.07.013. Fiber Supercontinuum sources and their applications
17. V.V. Alexander, O.P. Kulkarni, M. Kumar, C. Xia, M.N. Islam, F.L.T. Jr., M.J. Welsh, K. Ke, M.J. Freeman, M. Neelakandan, A. Chan, Opt. Fiber Technol. **18**(5), 349 (2012). doi:10.1016/j.yofte.2012.07.014. Fiber Supercontinuum sources and their applications
18. J.M. Dudley, F. Dias, M. Erkintalo, G. Genty, Nat. Photonics **8**(10), 755 (2014)
19. S.B. Cavalcanti, G.P. Agrawal, M. Yu, Phys. Rev. A **51**, 4086 (1995). doi:10.1103/PhysRevA.51.4086
20. J.M. Dudley, S. Coen, Opt. Lett. **27**(13), 1180 (2002). doi:10.1364/OL.27.001180
21. K. Corwin, N. Newbury, J. Dudley, S. Coen, S. Diddams, B. Washburn, K. Weber, R. Windeler, Appl. Phys. B **77**(2–3), 269 (2003). doi:10.1007/s00340-003-1175-x
22. K.L. Corwin, N.R. Newbury, J.M. Dudley, S. Coen, S.A. Diddams, K. Weber, R.S. Windeler, Phys. Rev. Lett. **90**, 113904 (2003). doi:10.1103/PhysRevLett.90.113904
23. N.R. Newbury, B.R. Washburn, K.L. Corwin, R.S. Windeler, Opt. Lett. **28**(11), 944 (2003). doi:10.1364/OL.28.000944
24. B. Kibler, C. Michel, J. Garnier, A. Picozzi, Opt. Lett. **37**(13), 2472 (2012). doi:10.1364/OL.37.002472
25. D. Solli, G. Herink, B. Jalali, C. Ropers, Nat. Photonics **6**(7), 463 (2012)

26. S.T. Sørensen, O. Bang, B. Wetzel, J.M. Dudley, Opt. Commun. **285**(9), 2451 (2012). doi:10.1016/j.optcom.2012.01.030
27. S.T. Sørensen, C. Larsen, U. Møller, P.M. Moselund, C.L. Thomsen, O. Bang, J. Opt. Soc. Am. B **29**(10), 2875 (2012). doi:10.1364/JOSAB.29.002875
28. G. Agrawal, *Nonlinear Fiber Optics*, 5th edn. Optics and Photonics (Academic Press, 2012)
29. M.H. Frosz, T. Sørensen, O. Bang, J. Opt. Soc. Am. B **23**(8), 1692 (2006). doi:10.1364/JOSAB.23.001692
30. F. Abdullaev, S. Darmanyan, S. Bischoff, P. Christiansen, M. Sørensen, Opt. Commun. **108**(1–3), 60 (1994). doi:10.1016/0030-4018(94)90216-X
31. F.K. Abdullaev, S.A. Darmanyan, S. Bischoff, M.P. Sørensen, JOSA B **14**(1), 27 (1997)
32. M.R. Karim, B.M.A. Rahman, G.P. Agrawal, Opt. Express **23**(5), 6903 (2015). doi:10.1364/OE.23.006903
33. A. Schliesser, N. Picqué, T.W. Hänsch, Nat. Photonics **6**(7), 440 (2012)
34. J. Hult, J. Lightwave Technol. **25**(12), 3770 (2007). doi:10.1109/JLT.2007.909373
35. G. Kallianpur, *Stochastic Filtering Theory* (Springer, 1980)